Naval Research Laboratory
Stennis Space Center, MS 39529-5004

NRL/MR/7320--10-9305

Global Ocean Forecast System V3.0 Validation Test Report Addendum: Addition of the Diurnal Cycle

E.J. Metzger
P.G. Thoppil

Ocean Dynamics and Prediction Branch
Oceanography Division

O.M. Smedstad
D.S. Franklin

QinetiQ North America
Technology Solutions Group
Slidell, Louisiana

November 5, 2010

REPORT DOCUMENTATION PAGE

Form Approved
OMB No. 0704-0188

1. REPORT DATE *(DD-MM-YYYY)*
05-11-2010

2. REPORT TYPE
Memorandum Report

3. DATES COVERED *(From - To)*

4. TITLE AND SUBTITLE
Global Ocean Forecast System V3.0 Validation Test Report Addendum: Addition of the Diurnal Cycle

5a. CONTRACT NUMBER

5b. GRANT NUMBER

5c. PROGRAM ELEMENT NUMBER
0603207N

6. AUTHOR(S)
E.J. Metzger, P.G. Thoppil, O.M. Smedstad,* and D.S. Franklin*

5d. PROJECT NUMBER

5e. TASK NUMBER

5f. WORK UNIT NUMBER
73-5094-10-5

7. PERFORMING ORGANIZATION NAME(S) AND ADDRESS(ES)
Naval Research Laboratory
Oceanography Division
Stennis Space Center, MS 39529-5004

8. PERFORMING ORGANIZATION REPORT NUMBER
NRL/MR/7320--10-9305

9. SPONSORING / MONITORING AGENCY NAME(S) AND ADDRESS(ES)
Space & Naval Warfare Systems Command
2451 Crystal Drive
Arlington, VA 22245-5200

10. SPONSOR / MONITOR'S ACRONYM(S)
SPAWAR

11. SPONSOR / MONITOR'S REPORT NUMBER(S)

12. DISTRIBUTION / AVAILABILITY STATEMENT
Approved for public release; distribution is unlimited.

13. SUPPLEMENTARY NOTES
*QinetiQ North America, Technology Solutions Group, Slidell, Louisiana

14. ABSTRACT
This report documents the ocean model response of adding diurnal variations to the incoming shortwave radiation forcing applied to the Global Ocean Forecast System Version 3.0. This can have a large impact on near surface ocean temperature and mixed layer, especially in low wind conditions when the near surface ocean is strongly stratified. This so-called "afternoon effect" can warm the upper ocean forming a thin mixed layer, and have a profound impact on the sound speed profile and surface duct. Hindcasts of GOFS V3.0 show an improved representation of the near surface afternoon warming when compared to observations, although proper representation of the atmospheric forcing is crucial to accurately model this effect. Nonetheless, time series of observed and hindcast sea surface temperature and mixed layer depth show higher correlations when the diurnal cycle is included as opposed to when it is not included.

15. SUBJECT TERMS
Global Ocean Forecast System Version 3.0
Diurnal variations of shortwave radiation
Afternoon effect

16. SECURITY CLASSIFICATION OF:			17. LIMITATION OF ABSTRACT	18. NUMBER OF PAGES	19a. NAME OF RESPONSIBLE PERSON
					E. Joseph Metzger
a. REPORT	b. ABSTRACT	c. THIS PAGE	UL	19	19b. TELEPHONE NUMBER *(include area code)*
Unclassified	Unclassified	Unclassified			(228) 688-4762

Standard Form 298 (Rev. 8-98)
Prescribed by ANSI Std. Z39.18

1.0 INTRODUCTION

In the development phase of the HYbrid Coordinate Ocean Model (HYCOM), time scales shorter than one day in specific atmospheric forcing fields were intentionally not accounted for. This was accomplished by applying a 1-day running filter to the 3-hourly thermal forcing fields, i.e. air temperature and specific humidity at 2 m, and net surface shortwave and longwave radiation. (The wind stresses and velocities were not temporally filtered in this way.) This methodology was used in all climatologically-forced ocean model spin-ups and their interannual extensions. In addition, this daily filtering was applied to the thermal forcing fields for the hindcasts used in the Phase I and II Validation Test Reports (VTRs) of the Global Ocean Forecast System (GOFS) Version 3.0 (V3.0) (consisting of the 1/12º global HYCOM that employs the Navy Coupled Ocean Data Assimilation (NCODA)) (Metzger et al., 2008; Metzger et al., 2010).

The diurnal variations of the incident shortwave (solar) radiation can have a large impact on near surface ocean temperature and mixed layer, especially in low wind conditions when the near surface ocean is strongly stratified. This so-called "afternoon effect" can warm the upper ocean forming a thin mixed layer and have a profound impact on the sound speed profile and surface duct (e.g. Urick, 1983). When the solar radiation is zero during the night, the ocean surface cools and the associated mixing leads to the erosion of this warmer and thinner diurnal mixed layer. Thus, the inclusion of the forcing on diurnal time scales in an ocean model may lead to improved representation of the upper ocean temperature and nowcasts/forecasts of the acoustical environment. This report is an addendum to the GOFS V3.0 Phase I and II VTRs and describes the testing and evaluation related to the inclusion of the diurnal cycle.

Manuscript approved October 12, 2010.

2.0 METHODOLOGY

Two hindcasts are integrated with the GOFS V3.0 ocean model and assimilation scheme. One includes the diurnal cycle of net surface shortwave radiation (Hindcast 80.3) while the other does not (Hindcast 80.4). Both hindcasts span the three month period from March-May 2008. Since the 3-hourly fields from the Navy Operational Global Atmospheric Prediction System (NOGAPS) are not sufficient to resolve the diurnal cycle, the same daily averaged thermal forcing fields are used in each hindcast but in the former an analytic cycle based on the ratio of instantaneous and daily averaged clear sky radiation from Lumb (1964) is imposed upon the shortwave radiation. This is accomplished by setting HYCOM namelist variable dswflg = 1. (Diurnal variability is not imposed on any other input thermal forcing fields.) Hindcast 80.4 is identical to the hindcast used in the Phase II VTR (74.2) with the exception of some minor changes in the HYCOM source code and a small change in the layer structure. Thirty two layers are still used, but the very deepest layer (that is only active in the polar regions) was merged with the layer immediately above and a one meter thick layer was added at the surface to provide more resolution in the mixed layer. We compared hindcasts 74.2 and 80.4 and found no significant differences associated with these ocean model software or layer structure modifications.

One important aspect of the validation of a system that includes the diurnal cycle is the need to compare each hindcast with the observations at the appropriate time of day. This is illustrated in Figure 1 that shows the GOFS V3.0 diagnostic mixed layer depth (MLD) difference between two time points twelve hours apart. The diagnostic MLD is defined as the density increase equivalent to a 0.3°C change in temperature from the surface to a given depth. In the hindcast without the diurnal cycle (top panel) the differences are generally small across the globe. Mixing associated with the movement of atmospheric fronts can be seen as red streaks (e.g. near 25°W, 35°S). With the inclusion of the diurnal cycle (bottom panel), regions with large MLD differences are evident between the two times and these are associated with the near surface afternoon warming. In the Pacific basin, mixed layers will be deepest at night (12Z) that corresponds to the seasonal MLD, and hence there are large negative differences (~20-50 m) when compared to 00Z (local noon); the opposite is true for the western Indian Ocean. It must also be noted that strong winds may sufficiently mix the water column enough to mask the afternoon warming and this is part of the reason why the largest MLD differences are seen in the tropical latitudes and not at mid-latitudes and poleward. Additionally, any afternoon warming will be small outside the tropics because of the time of year of the hindcasts (March-May). Given this potential for large diurnal variability in MLD, hindcast output and observations must be nearly contemporaneous. Output from both hindcasts is saved every three hours. In the validation, observations ±1.5 hours are considered contemporaneous, i.e. for the 03Z time point, observations between 1.5Z and 4.5Z are used in the error analyses.

3.0 DIURNAL CYCLE ERROR ANALYSES

The first analysis is simply to determine how well the near-surface afternoon warming is depicted in hindcast 80.3. This is shown in Figure 2 that is a time series during March 2008 of temperature in the upper 80 m for the two hindcasts and a Tropical Ocean Atmosphere (TAO) buoy located at 137°E, 5°N, within the western Pacific warm pool. This and other buoy-based observations used in this addendum are obtained from http://tao.noaa.gov. The observations (bottom panel) show afternoon warming extending down to ~20 m on most days. A comparison of wind speed and shortwave radiation during the period indicates the stronger warming events (e.g. March 3rd or 18th) coincide with weak winds and high shortwave radiation (as depicted in

Figures 3c and 3d, respectively). The middle panel in Figure 2 is hindcast 80.3 and the diurnal cycle is clearly seen in the ocean model response except that the afternoon warming extends to significantly deeper depths, ~80 m. This is due to the GOFS V3.0 layer structure in the warm pool area. Only the top three layers are in pressure (z) coordinates and these extend down to ~11 m. Below this is the much thicker (~80 m) first isopycnal layer. When the afternoon warming breaks through the pressures coordinates, the vertical extent is much deeper than observed because of this first relatively thick isopycnal layer. It should be noted that in most other parts of the world ocean (i.e. not in the warm pool), more pressure coordinates typically extend a bit deeper into the near surface water column. Hindcast 80.4 (top panel of Figure 2) shows no evidence of the afternoon warming. The overall pattern of the afternoon warming is consistent across the other buoys that we examined in this part of the world ocean at this time of year.

Additionally, Figure 3a and 3b show time series of MLD and sea surface temperature (SST). Hindcast 80.3 more closely tracks the observations than does hindcast 80.4, but there can still be significant differences. A large part of these differences can be explained in light of the differences in atmospheric forcing and two such examples are highlighted by the black vertical lines. On March 3rd the TAO buoy shows strong afternoon warming associated with higher (lower) observed net surface shortwave (winds) than by the NOGAPS analysis. Thus the observed MLD (SST) is shallower (higher) than hindcast 80.3. On March 25th, the opposite situation occurs where the NOGAPS shortwave radiation is higher than observed but the winds are nearly the same and hindcast 80.3 has shallower (higher) MLD (SST) than observed. In another example the difference in wind speed during 17-18 March explains the SST and MLD differences, i.e. a somewhat stronger NOGAPS wind speed is responsible for cooler SST and deeper MLD. Overall the NOGAPS peak shortwave radiation is less than observed while the wind speeds are comparable, except with fewer low wind conditions; this is generally true for all the western equatorial Pacific buoys examined. These examples highlight the importance of accurate atmospheric forcing in order to obtain the proper ocean model response. However, NOGAPS is unable to resolve the sub grid scale processes (less than 0.5°) that are the cause of some of this variability (e.g. convective thunderstorms). Hindcast and observed MLD and SST differences may also be the result of differences in horizontal advection.

Figure 4 shows a few additional MLD and SST time series comparisons between buoys and the hindcasts and the correlations are tabulated in Table 1. We concentrate on observations located in the tropics because the potential for afternoon warming should be largest there given the time of year. Again, hindcast 80.3 exhibits large diurnal variability that is similar in phase to the observations, but sometimes different in magnitude and this is likely attributed to differences in the atmospheric forcing (or advection). In all examples, the correlation between the observations and hindcast 80.3 is higher than the correlation with hindcast 80.4.

Table 1: Correlation coefficients between the observed and hindcast time series of MLD and SST for March 2008 at selected locations in the tropical ocean. Those highlighted in green have higher correlation coefficients.

Buoy Location	MLD		SST	
	Observations vs. 80.3	Observations vs. 80.4	Observations vs. 80.3	Observations vs. 80.4
137°E, 5°N	0.28	0.11	0.37	0.00
156°E, 0°N	0.52	0.24	0.54	0.28
165°E, 8°S	0.33	0.23	0.62	0.48
23°W, 0°N	0.15	0.02	0.46	0.38

Thus far the error analyses have focused on a few equatorial buoys with thermistor chains. However, Argo profiling floats can also be used in the analysis as these cover a wider geographic area. Nonetheless we still limit the analysis to tropical latitudes, i.e. region MER3c as defined in the Phase I VTR (Metzger et al., 2008). As the Argo profilers near the surface the last temperature measurement they take is typically near 8 m depth and this value is assumed constant to the surface since it should be well within the mixed layer. For the entire March-May 2008 period, we compare observed and hindcast temperature at 8 m depth using *unassimilated* Argo profile floats (Figure 5). This analysis shows that the inclusion of the diurnal cycle does not improve near surface temperature, but equally important it does not degrade the upper ocean.

Table 2: An acoustical proxy error analysis for mixed layer depth (MLD), sonic layer depth (SLD) and below layer gradient (BLG) using unassimilated profiles for the period March-May 2008. These acoustic variables are defined in the Phase I VTR (Metzger et al., 2008).Those highlighted in green have lower mean error and RMSE.

Variable	Number of unassimilated profiles	Mean from observations	Mean Error		RMSE	
			Hindcast 80.3	Hindcast 80.4	Hindcast 80.3	Hindcast 80.4
Region: MER3c						
MLD	4656	37.2 m	-0.7 m	-2.3 m	23.4 m	22.4 m
SLD	4195	48.8 m	-3.2 m	-6.6 m	26.0 m	24.9 m
BLG	4655	7.1 m/s/100 ft	-0.2 m/s/100 ft	-0.4 m/s/100 ft	2.5 m/s/100 ft	2.4 m/s/100 ft
Region: Arabian Sea						
MLD	245	16.5 m	2.6 m	5.0 m	13.3 m	15.3 m
SLD	145	32.8 m	-0.7 m	-7.7 m	18.7 m	21.4 m
BLG	245	5.3 m/s/100 ft	0.1 m/s/100 ft	-0.1 m/s/100 ft	2.1 m/s/100 ft	2.1 m/s/100 ft
Region: Western equatorial Pacific						
MLD	708	51.2 m	0.2 m	-4.0 m	32.3 m	29.6 m
SLD	693	68.1 m	1.3 m	-4.0 m	35.8 m	32.5 m
BLG	708	3.9 m/s/100 ft	0.2 m/s/100 ft	-0.2 m/s/100 ft	3.0 m/s/100 ft	2.8 m/s/100 ft

An acoustical proxy error analysis is also performed similar to the previous VTRs, but here it is limited to those regions where the afternoon warming might be expected to have the largest influence on the upper ocean. These are regions MER3c (±20° from the equator), the Arabian Sea (45-80°E, 0-24°N) and the western equatorial Pacific warm pool (140-180°E, 20°S-

20°N) and the results are tabulated in Table 2. In all regions the mean error (bias) is improved in the hindcast with the inclusion of the diurnal cycle or it is equal to the hindcast without it. Overall the bias is small relative to the mean of each variable. The largest improvement is in the Arabian Sea, an area that has been noted in the past two VTRs to be problematic. The RMSE is also lower in the Arabian Sea region, although it is slightly higher in the other two regions.

4.0 SUMMARY AND RECOMMENDATION

This addendum to the GOFS V3.0 Phase I and II VTRs focuses on the addition of the diurnal cycle to the net surface shortwave radiation and the ocean model response to this high frequency atmospheric forcing. Strong shortwave radiation (especially in low wind conditions) can significantly warm the near surface waters and have a profound impact on the sound speed profile and surface duct, i.e. the so-called "afternoon effect". Thus, proper representation of the diurnal cycle should lead to more accurate upper ocean temperature and nowcasts/forecasts of the acoustical environment.

Two 3-month hindcasts spanning March-May 2008 are integrated that include (80.3) and exclude (80.4) the diurnal cycle on shortwave radiation. This report focuses on those regions where the afternoon warming would be expected to have the highest impact, i.e. the tropical latitudes. The observations indicate the afternoon warming extends down to ~20 m. The near surface warming is clearly seen in hindcast 80.3 that includes the diurnal cycle, but it extends downward to deeper depths in part because of the model's layer structure in the western Pacific warm pool. Nonetheless, time series of MLD and SST show a much improved diurnal cycle when compared with observations and in all cases hindcast 80.3 produces higher correlation coefficients than hindcast 80.4. MLD and SST differences between the observations and hindcast 80.3 can often be attributed to differences in the observed and input shortwave radiation or wind forcing and this highlights the importance of accurate atmospheric forcing in order to obtain the appropriate ocean model response. An acoustical proxy error analysis also indicates that the bias is reduced in all the regions examined, especially the Arabian Sea that has been shown to be problematic in the past.

The addition of the diurnal cycle to the shortwave radiation forcing in GOFS V3.0 is an improvement over not including it and the upper ocean model response is clearly responding to the afternoon warming. Differences between observations and the hindcast are largely due to errors in the input atmospheric forcing or advection. It is therefore recommended that the diurnal cycle be included in the real-time GOFS V3.0 system running at NAVOCEANO.

5.0 ACKNOWLEDGEMENTS

This work was funded as part of the NRL 6.4 Large Scale Prediction and 6.4 Ocean Data Assimilation projects, managed by the Space and Naval Warfare Systems Command under program element 0603207N. The numerical simulations were performed on the Navy DoD Supercomputing Resource Center (DSRC) IBM Power 6 and Cray XT5 at Stennis Space Center, Mississippi using grants of computer time from the Department of Defense High Performance Computing Modernization Program.

6.0 REFERENCES

Lumb, F.E., 1964: The influence of clouds on hourly amounts of total solar radiation at the sea surface. *Quart. J. Roy. Meteor. Soc.*, **90**, 43-56.

Metzger, E.J., O.M. Smedstad, P.G. Thoppil, H.E. Hurlburt, A.J. Wallcraft, D.S. Franklin, J.F. Shriver and L.F. Smedstad, 2008: Validation Test Report for the Global Ocean Prediction System V3.0 - 1/12º HYCOM/NCODA: Phase I. *NRL Memo. Report*, NRL/MR/7320--08-9148.

Metzger, E.J., O.M. Smedstad, P.G. Thoppil, H.E. Hurlburt, D.S. Franklin, G. Peggion, J.F. Shriver T.L. Townsend and A.J. Wallcraft, 2010: Validation Test Report for the Global Ocean Forecast System V3.0 - 1/12º HYCOM/NCODA: Phase II. *NRL Memo. Report*, NRL/MR/7320--10-9236.

Urick, R.J., 1983: Principles of underwater sound, 3rd Edition. Peninsula Publishing, Los Altos, California, 423 pp.

7.0 TABLE OF ACRONYMS

BLG	Below Layer Gradient
DSRC	DoD Supercomputing Research Center
GOFS	Global Ocean Forecast System
HYCOM	HYbrid Coordinate Ocean Model
MLD	Mixed Layer Depth
NAVOCEANO	Naval Oceanographic Office
NCODA	Navy Coupled Ocean Data Assimilation
NOGAPS	Navy Operational Global Atmospheric Prediction System
NRL	Naval Research Laboratory
SLD	Sonic Layer Depth
SST	Sea Surface Temperature
TAO	Tropical Ocean Atmosphere
VTR	Validation Test Report

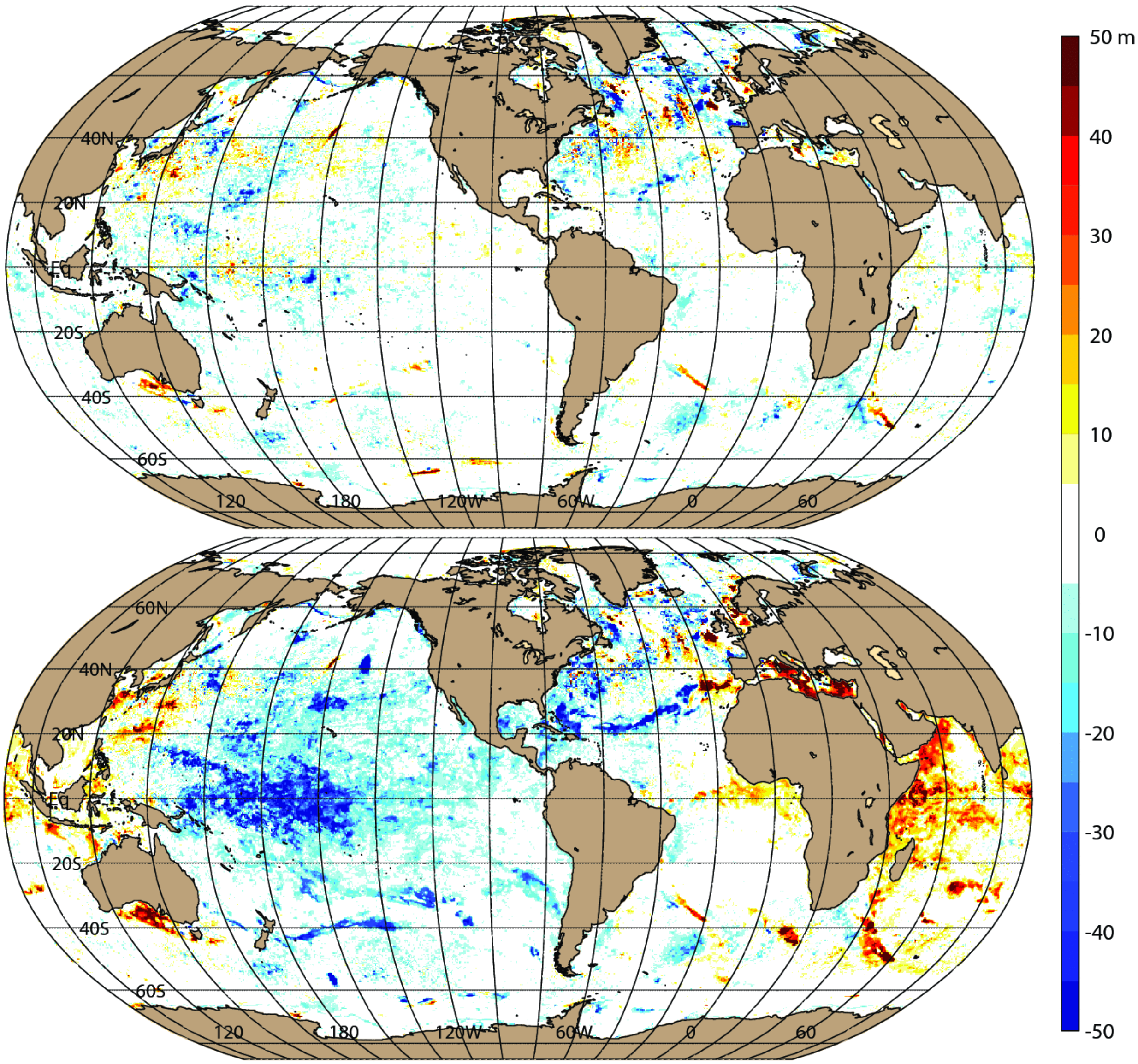

Figure 1: Mixed layer depth difference (in meters) between 15 March 2008 00Z and 15 March 2008 12Z for hindcast 80.4 without the diurnal cycle (top) and hindcast 80.3 with the diurnal cycle (bottom). Values that are less than ±5 m are white. The high/low pattern ~180° apart rotates around the globe relative to local noon/midnight.

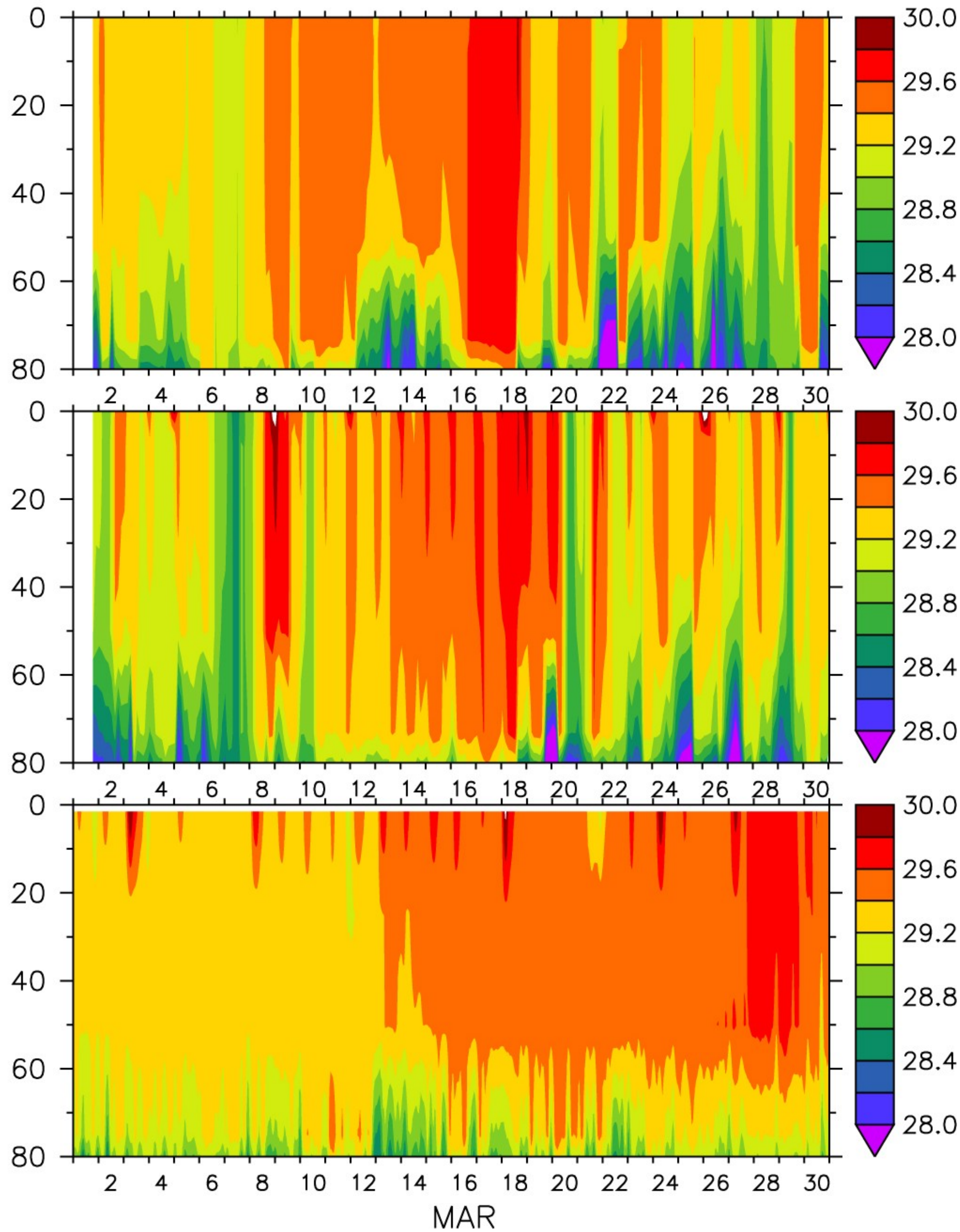

Figure 2: Temperature (°C) vs. depth as a function of time for March 2008 at 137°E, 5°N for hindcast 80.4 without the diurnal cycle (top), hindcast 80.3 with the diurnal cycle (middle) and observations from a TAO buoy (bottom). The tick marks at the bottom mark the beginning of each day and the numbers are marked at the middle of the day. The GOFS V3.0 output are 3-hourly whereas the TAO observations are 1-hourly.

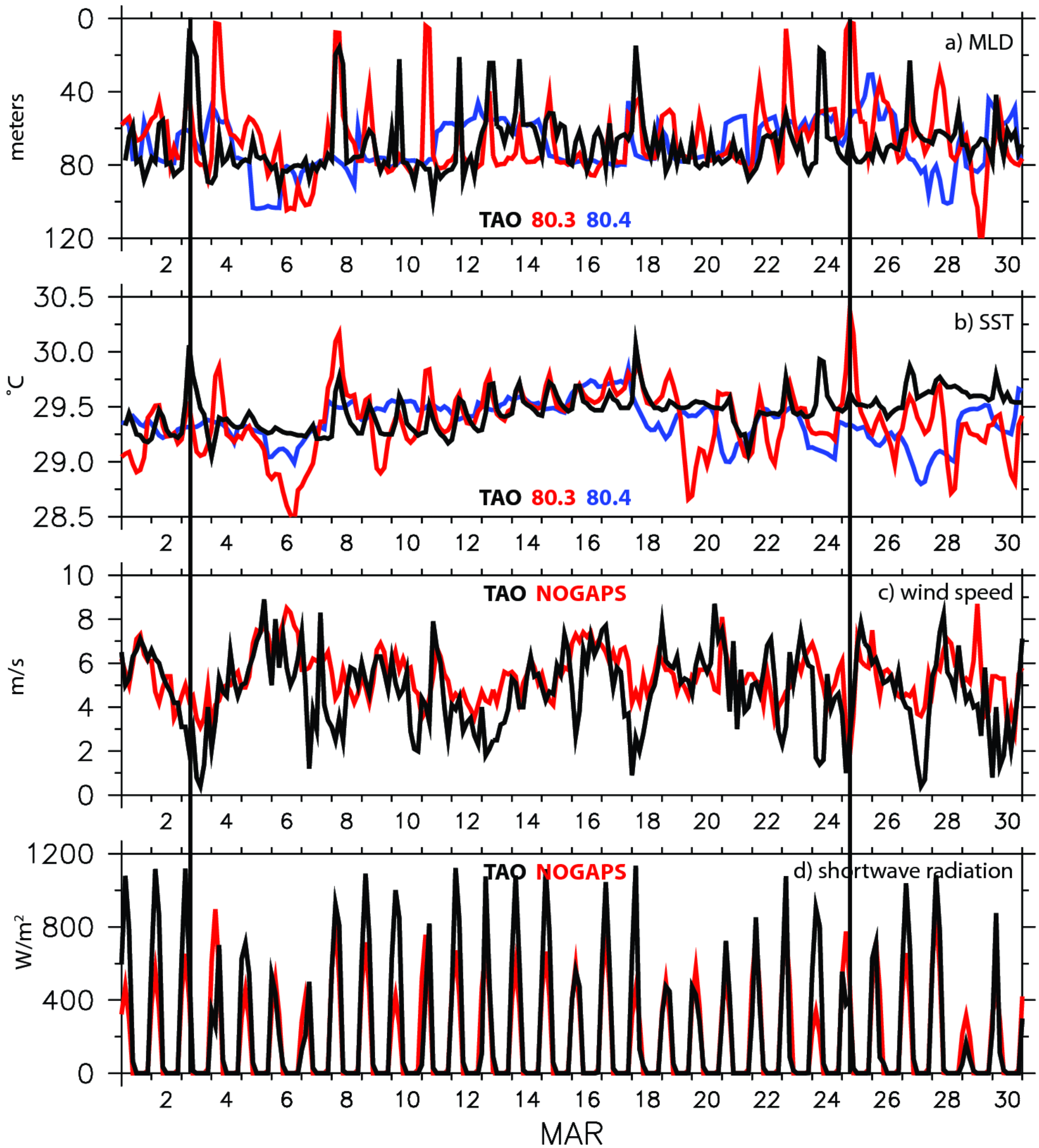

Figure 3: Time series for March 2008 at 137°E, 5°N for a) mixed layer depth (meters), b) sea surface temperature (°C), c) wind speed (m/s) and d) net surface shortwave radiation (W/m^2). In panels a, b the black curves are TAO observations, the red curves are hindcast 80.3 with the diurnal cycle and the blue curves are hindcast 80.4 without the diurnal cycle. In panels c, d the black curves are TAO observations and the red curves are from NOGAPS. All curves have 3-hourly temporal frequency.

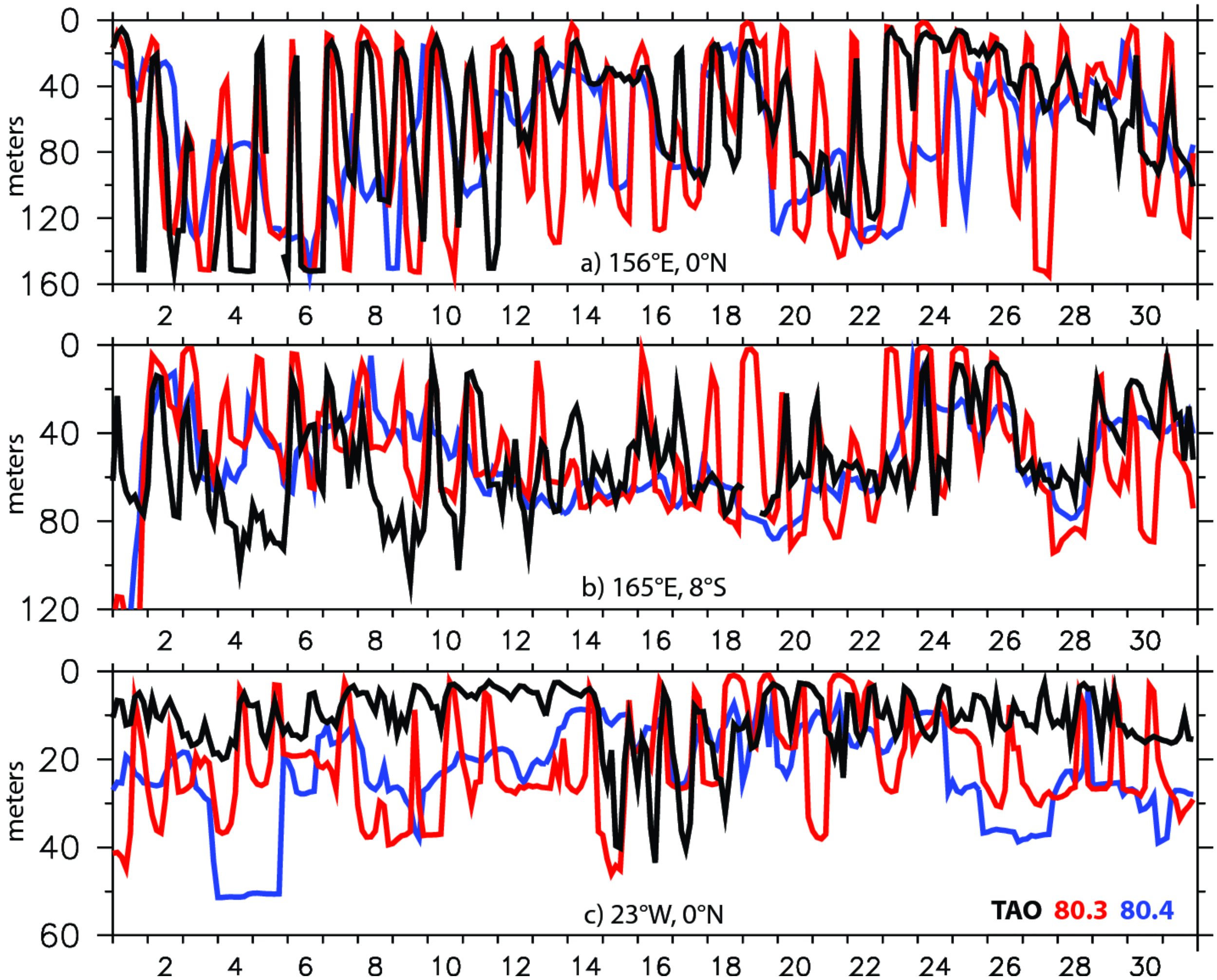

Figure 4: Time series of mixed layer depth (meters) for March 2008 at a) 156°E, 0°N, b) 165°E, 8°S and c) 23°W, 0°N. The black curves are TAO observations, the red curves are hindcast 80.3 with the diurnal cycle and the blue curves are hindcast 80.4 without the diurnal cycle. All curves have 3-hourly temporal frequency.

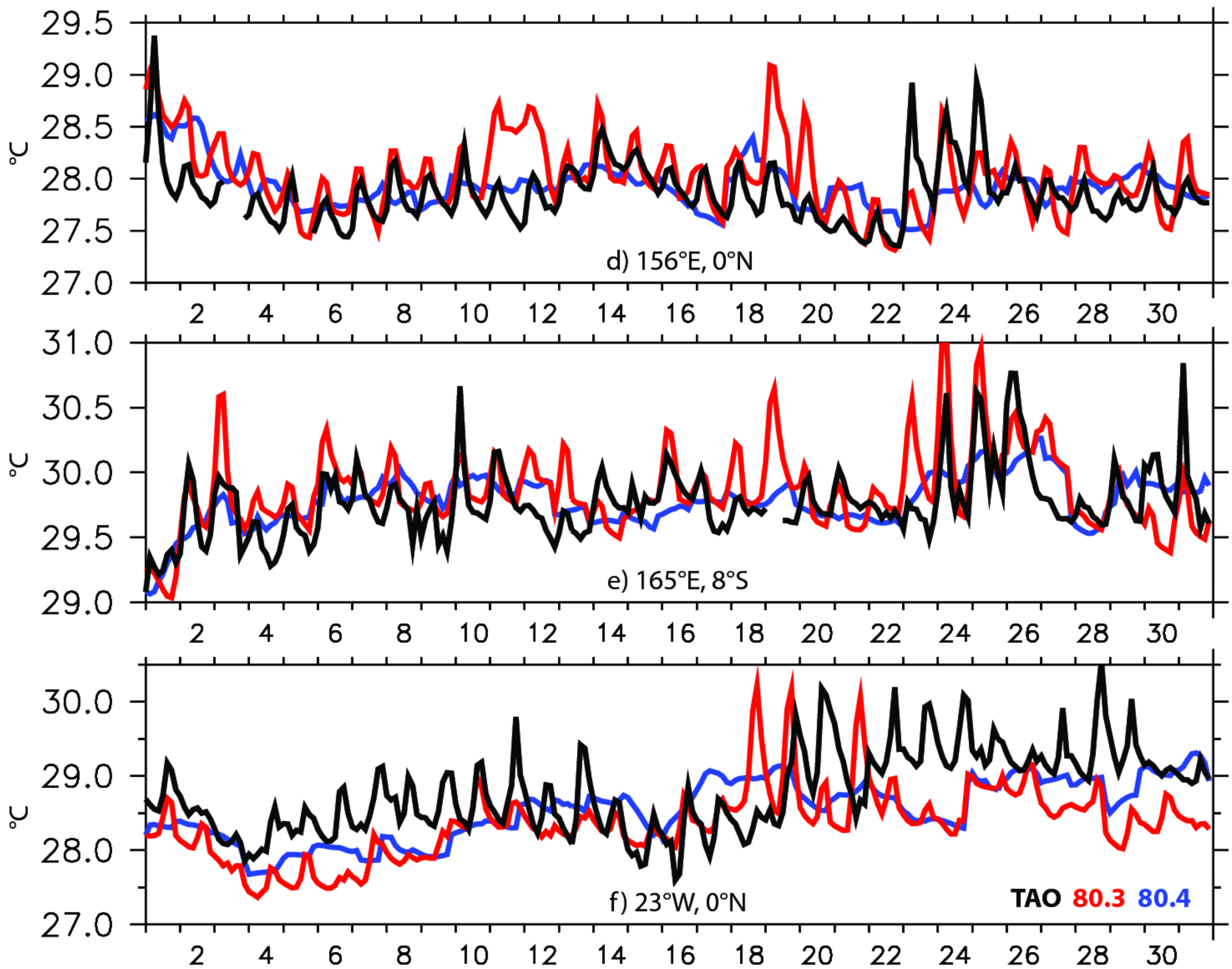

Figure 4 (continued): Time series of SST (°C) for March 2008 at d) 156°E, 0°N, e) 165°E, 8°S and f) 23°W, 0°N. The black curves are TAO observations, the red curves are hindcast 80.3 with the diurnal cycle and the blue curves are hindcast 80.4 without the diurnal cycle. All curves have 3-hourly temporal frequency.

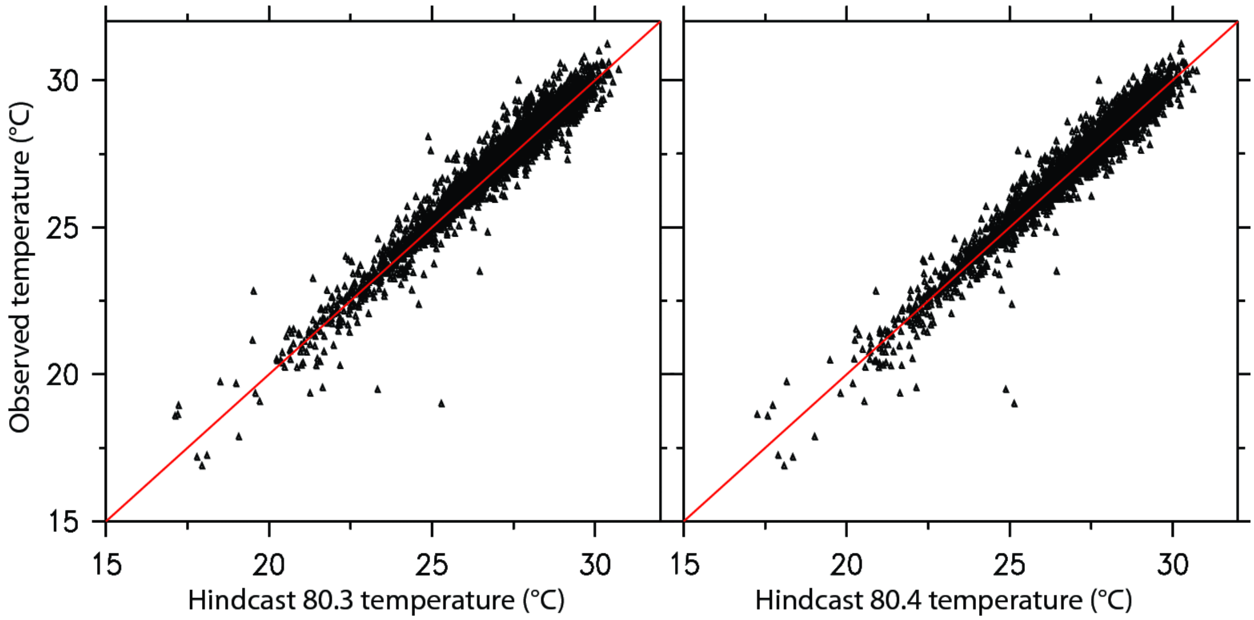

Figure 5: Scatterplot of observed vs. hindcast temperature (°C) at 8 m depth using 4510 unassimilated Argo profiling floats in the MER3c region over the period March-May 2008. Hindcast 80.3 (80.4) is on the left (right) and has a root mean square difference of 0.42°C (0.39°C).